

University of Wollongong

Research Online

Faculty of Engineering and Information
Sciences - Papers: Part B

Faculty of Engineering and Information
Sciences

2017

Reinforced concrete beams strengthened in flexure with near-surface mounted (NSM) CFRP strips: Current status and research needs

Shi Shun Zhang

University of Wollongong, shishun@uow.edu.au

Tao Yu

University of Wollongong, taoy@uow.edu.au

G M. Chen

Guangdong University of Technology

Follow this and additional works at: <https://ro.uow.edu.au/eispapers1>



Part of the [Engineering Commons](#), and the [Science and Technology Studies Commons](#)

Recommended Citation

Zhang, Shi Shun; Yu, Tao; and Chen, G M., "Reinforced concrete beams strengthened in flexure with near-surface mounted (NSM) CFRP strips: Current status and research needs" (2017). *Faculty of Engineering and Information Sciences - Papers: Part B*. 521.

<https://ro.uow.edu.au/eispapers1/521>

Research Online is the open access institutional repository for the University of Wollongong. For further information contact the UOW Library: research-pubs@uow.edu.au

Reinforced concrete beams strengthened in flexure with near-surface mounted (NSM) CFRP strips: Current status and research needs

Abstract

The near-surface mounted (NSM) FRP strengthening technique has attracted worldwide attention as an effective alternative to the externally bonded (EB) FRP strengthening technique. In the NSM FRP strengthening method, grooves are first cut in the concrete cover of a concrete member for the FRP reinforcement to be inserted and embedded using an adhesive. The NSM FRP method has many advantages over the EB FRP method, including a higher bonding efficiency and a better protection of the FRP reinforcement. Existing experimental studies have shown that FRP strips owned a better bond efficiency compared with other section shapes (e.g. round bars and square bars), due to the fact that they had a larger perimeter-to-cross-sectional area ratio. This paper presents a state-of-the-art review, particularly on the flexural strengthening of RC beams with NSM CFRP strips. The observed failure modes in laboratory experiments of such FRP-strengthened RC beams are classified and the existing strength models are examined along with the failure mechanisms behind. The main knowledge gaps to be bridged in future studies are also identified. This review partially formed the basis of the development of design provisions on the NSM strengthening technique in the relevant Hong Kong design guideline.

Disciplines

Engineering | Science and Technology Studies

Publication Details

Zhang, S., Yu, T. & Chen, G. M. (2017). Reinforced concrete beams strengthened in flexure with near-surface mounted (NSM) CFRP strips: Current status and research needs. *Composites Part B: Engineering*, 131 30-42.

Reinforced concrete beams strengthened in flexure with near-surface mounted (NSM) CFRP strips: current status and research needs

S.S. Zhang ^a, T. Yu ^{a,*}, G.M. Chen ^b

^a School of Civil, Mining & Environmental Engineering, Faculty of Engineering & Information Sciences, University of Wollongong, Northfields Avenue, Wollongong, NSW 2522, Australia.

^b School of Civil and Transportation Engineering, Guangdong University of Technology, Guangzhou 510006, China.

Abstract: The near-surface mounted (NSM) FRP strengthening technique has attracted worldwide attention as an effective alternative to the externally bonded (EB) FRP strengthening technique. In the NSM FRP strengthening method, grooves are first cut in the concrete cover of a concrete member for the FRP reinforcement to be inserted and embedded using an adhesive. The NSM FRP method has many advantages over the EB FRP method, including a higher bonding efficiency and a better protection of the FRP reinforcement. Existing experimental studies have shown that FRP strips owned a better bond efficiency compared with other section shapes (e.g. round bars and square bars), due to the fact that they had a larger perimeter-to-cross-sectional area ratio. This paper presents a state-of-the-art review, particularly on the flexural strengthening of RC beams with NSM CFRP strips. The observed failure modes in laboratory experiments of such FRP-strengthened RC beams are classified and the existing strength models are examined along with the failure mechanisms behind. The main knowledge gaps to be bridged in future studies are also identified. This review partially formed the basis of the development of design provisions on the NSM strengthening technique in the relevant Hong Kong design guideline.

Keywords: FRP, near-surface mounted (NSM), strip, RC beams

*Corresponding author. Email: taoy@uow.edu.au

34 **1 Introduction**

35 The externally bonded (EB) FRP method has become a prevailing technique over the last two
36 decades [e.g. 1-2] for the strengthening of existing reinforced concrete (RC) members. In the
37 past ten years, as a promising alternative to the EB FRP method, the near-surface mounted
38 (NSM) FRP strengthening technique has attracted increasing worldwide attention [e.g. 3-5].
39 In the NSM FRP strengthening method, grooves are first cut in the concrete cover of RC
40 members and FRP bars are then embedded into the grooves with an adhesive. FRP bars of
41 various cross-sectional shapes can be used in the NSM FRP strengthening method, such as
42 square, round, and rectangular bars (Fig. 1). The NSM FRP method owns many advantages
43 over the EB FRP method, including a higher bonding efficiency and a better protection of the
44 FRP reinforcement [e.g. 4].

45
46 De Lorenzis and Teng [4] provided a detailed and critical review of the research available to
47 them at that time on the strengthening of concrete structures with NSM FRP reinforcement.
48 Their review covered various aspects of the NSM FRP strengthening technique (e.g. FRP
49 reinforcement; construction aspects; bond) for various applications (e.g. flexural
50 strengthening; shear strengthening). De Lorenzis and Teng [4] also outlined the main
51 research needs for more extensive applications of this strengthening technique, with the bond
52 behaviour between NSM FRP bars and concrete being identified as an important issue to be
53 further examined. After De Lorenzis and Teng's work [4], a significant amount of research
54 has been conducted, including experimental [e.g. 6-20], theoretical [e.g. 14, 15, 19, 21-29]
55 and numerical [e.g. 9, 15, 30-32] studies into the behaviour of concrete structural members
56 strengthened with various NSM FRPs. More recently, Coelho et al. [5] conducted a review on
57 the bond behaviour of NSM FRP technique. Their review, however, was limited to the bond
58 behavior of NSM FRP-to-concrete bonded interfaces and did not cover the behavior of NSM

59 FRP-strengthened RC beams. In addition, Coelho et al.'s review [5] appears to be inadequate
60 in the sense that (1) it did not cover some of the debonding failure modes reported in the
61 existing literature [e.g. 7, 14, 19]; (2) it did not cover the recent advances in the development
62 of bond-slip models [e.g. 26, 33] and bond strength models which are important for a better
63 understanding of bond behaviour between NSM FRP and concrete.

64

65 One important finding by these more recent studies is that FRP strips (rectangular bars which
66 have a large bar height-to-thickness ratio) are superior to NSM FRP bars of other shapes in
67 terms of the bond performance [e.g. 5, 16, 19, 34, 35] and thus the strengthening efficiency
68 [e.g. 3, 5]. This is due to the fact that an FRP strip usually has a larger
69 perimeter-to-cross-sectional-area ratio and a larger embedment depth than an FRP bar of other
70 shapes, which consequently leads to a larger bond force between NSM FRP and surrounding
71 concrete and a higher utilization of the tensile capacity of FRP. Strips made of carbon FRP
72 (CFRP) are more attractive than other types of FRP for NSM strengthening applications due
73 to their high strength and stiffness which could lead to a small cross-sectional area. The
74 recent studies on NSM CFRP strips-strengthened concrete structures have led to much
75 improved understanding of and more rational theoretical models for such structures,
76 especially for those where CFRP strips are used for flexural strengthening. These studies have
77 also unpinned the first ever systematic design procedure for the NSM strengthening technique
78 in a design guideline [36] for which the authors are among the main contributors. Against this
79 background, this paper presents a state-of-the-art review on the flexural strengthening of RC
80 beams with NSM CFRP strips. This review partially formed the basis of the development of
81 design provisions on the NSM strengthening in the relevant Hong Kong design guideline
82 [36].

83

84 **2 Behaviour and debonding failure modes of RC beams strengthened in** 85 **flexure with NSM FRP**

86 *2.1 General Behaviour of NSM FRP-Strengthened RC Beams*

87 Many laboratory tests on RC beams strengthened with NSM round FRP bars or square FRP
88 bars have been conducted to investigate this promising technique [e.g. 3, 8, 37-41]. A
89 significant number of experimental studies have also been conducted on RC beams
90 strengthened in flexure with NSM CFRP strips (referred to as NSM CFRP RC beams
91 hereafter for simplicity) in the past two decades [e.g. 3, 20, 42-56]. The existing experimental
92 studies on NSM CFRP RC beams generally show a significant enhancement of the flexural
93 capacity of the strengthened RC beam, with the maximum percentage increase in the flexural
94 capacity being more than 200%. The exact amount of enhancement depends on the amount of
95 FRP, the steel reinforcement ratio and the failure mode, among others. Compared to the
96 results of RC beams strengthened with externally bonded FRP plates (referred to as
97 FRP-plated RC beams hereafter for simplicity), a much higher utilization of the tensile
98 capacity of the FRP was observed in NSM CFRP RC beams [e.g. 3, 20, 44, 48, 50].
99 Furthermore, similar to the observation from bonded joint tests [e.g. 34, 35], NSM CFRP
100 strips showed much higher bond efficiency than NSM FRP round bars in NSM CFRP RC
101 beams [e.g. 3], owing to the higher perimeter-to-cross-sectional area ratio of the former.

102

103 From the load-deflection curves at the mid-span of most NSM CFRP RC beams, it was
104 shown that NSM CFRP strips did not contribute much to the flexural stiffness of the beam in
105 the elastic stage (i.e. before concrete cracking). After cracking, however, the flexural stiffness
106 of the beam can be significantly increased compared with an un-strengthened beam. The
107 flexural strength as well as the ductility of NSM CFRP RC beams was much higher than
108 FRP-plated RC beams [e.g. 3, 44]. Using U-shaped FRP/steel jackets for end anchorage of

109 NSM CFRP strips was shown to postpone the debonding failure of FRP and thus
110 significantly improve the ductility of the beam, although the increase in the flexural capacity
111 was not apparent [e.g. 50, 54, 57]. Information on the effect of U-shaped jacketing on the
112 effectiveness of NSM FRP used for flexural strengthening, however, is very limited.

113 **2.2 Debonding failure modes**

114 Despite a relatively strong bond between NSM CFRP strips and concrete, debonding failures
115 are still likely to happen in RC beams strengthened in flexure with NSM CFRP strips. In the
116 context of simply-supported NSM CFRP RC beams, debonding failure modes are likely to
117 occur both at the ends of NSM CFRP strips and in the maximum moment region. Apart from
118 interfacial debonding that occurs at or near a bi-material interface, debonding may also occur
119 in the form of separation of concrete cover where the concrete cover containing the NSM
120 CFRP strips are detached along the level of the steel tension bars. In this paper, the term
121 “debonding” refers to both interfacial debonding failure and cover separation failure; that is,
122 it refers to all failure modes where the composite action between the FRP and the concrete
123 beam is not maintained. In the experimental studies of NSM CFRP RC beams, in addition to
124 the two conventional failure modes of RC beams, namely, flexural failure by crushing of
125 compressive concrete [e.g. 47, 49, 58] and flexural failure by rupture of FRP [e.g. 3, 42], the
126 following debonding failure modes have been reported:

127 1) ***Intermediate crack induced debonding (referred to as IC debonding hereafter) failure***
128 [e.g. 49, 50]. In this failure mode, the debonding of the CFRP strip starts from the
129 maximum moment region and propagates to one of the FRP strip ends. A typical
130 schematic diagram of the IC debonding failure is illustrated in Fig. 2. As can be seen
131 from Fig. 2, the IC debonding failure can be further divided into two sub-types: ***IC***
132 ***interfacial debonding*** [50] and ***IC cover separation*** [49]. In the IC interfacial debonding,
133 the debonding happens between the CFRP strip and the surrounding concrete (more

134 accurately, in the thin concrete layer adjacent to the adhesive layer). In the IC cover
135 separation failure, the CFRP strip together with the concrete cover is detached from the
136 beam starting from the maximum moment region, with a major crack travelling on the
137 plane of the steel tension bars; and

138 2) **End debonding failure** [e.g. 42-45, 51, 54, 59]. In this failure mode, the debonding of
139 the CFRP strip starts from one end of the FRP strip and propagates to the mid-span of the
140 beam. This failure mode is mainly due to the high interfacial shear and normal stresses
141 caused by the abrupt termination of the CFRP strip [23, 29]. A typical schematic of the
142 end debonding failure is illustrated in Fig. 3. As can be seen from Fig. 3, the end
143 debonding failure can also be further divided into two sub-types: **end interfacial**
144 **debonding** [e.g. 42, 54] and **end cover separation** [e.g. 20, 43-45, 51-53]. Except for
145 the starting points of the debonding, end interfacial debonding and end cover separation
146 are quite similar to their counterparts IC interfacial debonding and IC cover separation
147 respectively.

148

149 While the above failure modes were reported in the existing literature, some researchers only
150 indicated that failure of the beam was caused by concrete cover separation but did not
151 mention where the failure initiated [e.g. 48, 52]. Among the above debonding failure modes,
152 cover separation (i.e. IC cover separation and end cover separation) has been found to be
153 more common than interfacial debonding (i.e. IC interfacial debonding and end interfacial
154 debonding) in NSM CFRP RC beams. Possible reasons for this phenomenon include: (1) the
155 strong bond between NSM CFRP strips and concrete makes the interfacial debonding failure
156 less likely; and (2) the large radial stresses, exerted by the steel tension bars to the
157 surrounding concrete during their tension process [31], plays an important role in accelerating
158 the cracking in the concrete along the level of steel tension bars. Nevertheless, interfacial

159 debonding is also an important debonding failure mode, especially for NSM
160 FRP-strengthened RC beams with a relatively large beam width [28]. The present paper aims
161 to clarify the failure mechanism of the above debonding failure modes, to summarize the
162 established strength models and to identify the gaps of knowledge for future research.

163

164 **3 IC debonding**

165 Although IC interfacial debonding and IC cover separation are both termed as debonding
166 failure, the intrinsic failure mechanisms of them are quite different. The interfacial debonding
167 failure happens on the NSM CFRP strip-to-concrete interfaces and the debonding strength is
168 thus mainly controlled by the material and/or interfacial properties on/near such interfaces.
169 Obviously, in order to find out the debonding mechanism and establish strength models for
170 interfacial debonding failures in NSM CFRP RC beams, the fundamental issue is to expose
171 the bond behaviour of the NSM CFRP strip-to-concrete interface. In contrast, the cover
172 separation failure happens on the horizontal plane of tension steel bars with both concrete
173 cover and FRP detached from the RC beam. Therefore, in order to establish the strength
174 models for cover separation failures in NSM CFRP RC beams, one of the fundamental issues
175 is to clarify the failure mechanism on the horizontal plane of tension steel bars.

176 **3.1 IC Interfacial Debonding**

177 *3.1.1 Failure mechanism*

178 The failure process and mechanism of IC interfacial debonding is usually as follows: when a
179 dominating flexural crack occurs in/near the maximum moment zone, the tensile stress in the
180 concrete releases and is transferred onto the tension steel bars as well as FRP reinforcement
181 through interfacial shear stresses. Near the intersection of FRP reinforcement and the
182 dominating flexural crack, high local interfacial shear stresses happens as a result of the
183 geometric discontinuity of concrete due to the existence of the flexural crack. These high

184 local interfacial shear stresses increase as the applied load increases and finally result in the
185 initiation of debonding between FRP and concrete while it reaches a critical level. Afterwards,
186 the IC interfacial debonding process is mainly driven by the opening of the flexural crack
187 which causes relatively displacements between FRP and concrete. The propagation of
188 debonding therefore strongly depends on the bond behaviour of NSM CFRP strip-to-concrete
189 interfaces, which can be investigated through the tests of NSM CFRP strip-to-concrete
190 bonded joints as shown in Fig. 4. In other words, the findings from such bonded joints has the
191 potential to be used for predicting the force (stress) that can be developed in the NSM CFRP
192 strip at IC interfacial debonding. In the following subsections, the existing studies on NSM
193 CFRP-concrete bonded joints/interfaces are first reviewed based on which recommendations
194 on the bond strength of IC interfacial debonding in an NSM CFRP RC beam are provided.

195 *3.1.2 Behaviour of NSM CFRP strip-to-concrete interfaces*

196 The interfacial bond behaviour has been commonly studied using pull-out tests on NSM
197 FRP-to-concrete bonded joints. By far, the beam pull-out test and the direct pull-out test have
198 been adopted by existing studies to study the bond behavior between NSM FRP bars and
199 concrete. The former one had been widely used for the study of the bond characteristics of
200 steel bars and was introduced by Nanni et al. [60] for NSM FRP bars. The later one has three
201 main sub-types: one-side pull-out test [e.g. 6, 21, 45, 61, two-side pull-out test [e.g. 62], and
202 C-shaped block pull-out test [e.g. 37, 38]. As the one-side pull-out test is the simplest one to
203 be implemented in laboratory experiments and its loading mechanism is direct and clear, it
204 has been the most common test method adopted by researchers.

205

206 *Failure modes*

207 A number of failure modes have been observed in experimental studies of NSM CFRP
208 strip-to-concrete bonded joints, including: (1) adhesion failure on the strip-to-adhesive

209 interface [18, 19, 58, 61, 63, 54]; (2) adhesion failure on the adhesive-to-concrete interface
210 [14, 18, 19, 34, 35, 64]; (3) cohesion failure in a thin layer of concrete near the
211 adhesive-concrete interface [6, 7, 14, 18, 19, 21, 63-66]; (4) cohesion failure in the adhesive
212 [7, 16, 34, 61]; (5) splitting of the concrete block [7]; and (6) rupture of FRP strip [14, 18, 19].
213 Among these failure modes, the splitting of concrete block only happened in the specimens
214 where the CFRP strips were deliberately embedded much deep in concrete blocks [7]. This
215 failure mode is therefore unlikely to occur in RC beams as the embedment depth of FRP
216 strips in RC beams is generally limited by the thickness of concrete cover. The rupture of
217 FRP strip depends on the tensile strength of FRP and is thus not a property of the bonded
218 interface. The adhesion failure at strip-to-adhesive or adhesive-to-concrete interfaces is
219 largely a result of the poor surface condition at the corresponding interface (e.g. the surface
220 of the CFRP strip or groove is not well cleaned) while the cohesion failure in the adhesive
221 generally occurs when a weak adhesive is used or when the adhesive thickness is too small so
222 that the stress concentration in the adhesive layer is significant. These three failure modes are
223 not the desired failure modes as the failure occurs in the strengthening system and thus the
224 strengthening efficiency would be significantly compromised. Indeed, these failure modes
225 should be avoided in the design by a proper groove size, an appropriate treatment of the
226 interfaces and selection of adhesives. Therefore, existing studies [4, 67] have suggested that
227 the preferred failure mode is cohesion failure in a thin layer of the concrete near the
228 adhesive-to-concrete interface. With such failure mode, the bond strength is governed largely
229 by the concrete properties but not the properties on the adhesive-to-concrete interface or the
230 CFRP-to-adhesive interface, so the development of a design theory is also easier. A few
231 bond-slip and bond strength models have been proposed for this failure mode and are
232 discussed later in this section.

233

234 Bond-slip models

235 An accurate bond-slip model for the NSM CFRP strip-to-concrete interface is crucial to an
236 in-depth understanding of debonding failures in NSM FRP-strengthened RC members, and is
237 necessary for developing accurate bond strength models for NSM CFRP strip-to-concrete
238 interfaces. In addition, an accurate bond-slip model is critical to establishing accurate finite
239 element models of NSM FRP-strengthened RC members for predicting debonding processes.
240 Compared to bond-slip models developed for EB FRP laminate/plate-to-concrete interfaces
241 [e.g. 68, 69], existing work on bond-slip models for NSM FRP strip-to-concrete interfaces is
242 still relatively limited. Similar to EB FRP systems, the bond-slip model for NSM
243 FRP-to-concrete interfaces can be developed using experimental approaches (i.e., direct
244 regression of experimental results) [e.g. 21, 38, 70] or numerical parametric studies [e.g. 69].
245 When the experimental approach is adopted, the bond-slip model may be determined from
246 axial strain distributions of the CFRP bar obtained by strain instruments [37] or from the
247 average bond stress versus average slip (obtained from loaded-end slip and free-end slip)
248 curve [e.g. 38]. The large scatter of test results as a result of the heterogeneity of concrete [4]
249 may influence the accuracy of the proposed bond-slip curves. In addition, the bond behaviour
250 on the FRP-to-adhesive interface might be interfered by the installation of strain gauges for
251 the strain measurement. By far, four bond-slip models have been proposed by De Lorenzis
252 and her co-workers [38, 71-73] for NSM FRP round bars-to-concrete interface based on the
253 test results. However, these bond-slip models cannot be directly applied to NSM CFRP
254 strip-to-concrete interfaces. The stress state in the adhesive and the surrounding concrete is
255 relatively complicated for NSM FRP round bars than for NSM FRP strips especially when
256 ribbed bars/spirally wounded bars are used. For NSM CFRP strip-to-concrete interface, a
257 bond-slip model was proposed by Sena-Cruz and Barros [74], based on a model adopted for
258 steel bar-to-concrete interfaces [75]; their model was calibrated with their tests in which the

259 concrete was deliberately strengthened with steel fibres to avoid failure in the concrete. The
 260 bond-slip model adopted by CEB-FIP [76] for steel bar-to-concrete interfaces was
 261 recommended by Borchert and Zilch and the linear-softening bond-slip model which has the
 262 same form as that for EB FRP-to-concrete interface was used by Seracino et al. [21] for NSM
 263 CFRP strip-to-concrete interface. The validity of the above models is still uncertain in the
 264 sense that they were based on previous work on steel bar-to-concrete interfaces or on EB FRP
 265 reinforcements but not directly deduced from experimental tests or verified numerical
 266 simulations. However, the proposals of these bond-slip models provide useful attempts and
 267 help to some extent understand the bond behaviour of NSM CFRP strip-to-concrete interfaces.
 268 More recently, using the verified 3-D meso-scale FE model proposed by Teng et al. [67, 77],
 269 Zhang et al. [26] conducted a parametric study to examine the bond-slip relationship on NSM
 270 CFRP strip-to-concrete interfaces. It was found from the study that: (1) the bond-slip curve
 271 has a nonlinear ascending branch with the slope continuously decreasing; (2) the descending
 272 branch is also nonlinear with the magnitude of the slope increasing first and then decreasing
 273 with the increase of slip; (3) the ascending and descending branches are smoothly connected.
 274 Finally they proposed the bond-slip relationship (Eq. 1) for such bonded interfaces with the
 275 currently preferred failure mode (i.e. cohesion failure in the concrete near the
 276 adhesive-concrete interface), in which the concrete cylinder strength (f_c) and the groove
 277 height (h_g)-to-width (w_g) ratio were finally selected as the two key parameters that
 278 influence the bond behaviour.

$$279 \quad \tau = A \left(\frac{2B-s}{B} \right)^2 \sin \left(\frac{\pi}{2} \cdot \frac{2B-s}{B} \right) \quad \text{with} \quad s \leq 2B \quad (1)$$

280

281 where τ is the bond stress, s is the slip, $A = 0.72\gamma^{0.138} f_c^{0.613}$ and $B = 0.37\gamma^{0.284} f_c^{0.006}$,

282 $\gamma = \frac{h_g}{w_g}$ is the groove height to-width ratio and f_c is the cylinder compressive strength of
 283 concrete.

284

285 Bond strength models

286 The bond strength is the ultimate tensile force that can be developed in the FRP
 287 reinforcement in a pull-out test before the debonding between FRP and concrete occurs. It has
 288 been found in existing studies [e.g. 6, 63] that the bond strength of NSM CFRP
 289 strip-to-concrete interface increases with when the bond length is relatively small, but when
 290 the bond length exceeds a threshold value, a further increase in the bond strength cannot be
 291 obtained from a further increase in the bond length. The threshold value of bond length has
 292 been referred to as the effective bond length (L_e) [e.g. 78, 79]. The fracture mechanics-based
 293 approaches [78, 81] can well interpret the existence of an effective bond length and can be
 294 used to establish the bond strength based on a given bond-slip curve [80, 81]. By now, four
 295 bond strength models of NSM CFRP-to-concrete interfaces have been proposed for the
 296 currently preferred failure mode. They are introduced below.

297

298 *Seracino and co-workers' model [7, 21, 65]*

299 Based on their test results, Seracino and co-workers [7, 21, 65] proposed a bond strength
 300 model for cohesion failure in a thin layer of concrete near the adhesive-to-concrete interface
 301 (referred to as debonding in Refs. [7], [21] and [65]). In this model, the bond strength $P_{u,s}$ of
 302 NSM CFRP strip-to-concrete interface is expressed as

$$303 \quad P_{u,s} = \alpha_p 0.85 \beta_e \beta_{L,s} \gamma_s^{0.25} f_c^{0.33} \sqrt{E_f A_f L_{failure} \left(\frac{h_f + c_a}{c_a} \right)^{1.2}} \quad (2)$$

$$\alpha_p = \begin{cases} 1 & \text{for the mean value} \\ 0.85 & \text{for the 95\% lower bound} \end{cases} \quad (3)$$

$$\beta_e = 0.283 \frac{a_e}{h_f} + 0.196 \leq 1 \quad (4)$$

$$\beta_{L,s} = \frac{L_b}{L_{e,s}} \leq 1 \quad (5)$$

$$L_{e,s} = \frac{\pi}{2(0.802 + 0.078)} \sqrt{\frac{0.976 \gamma_s^{0.526} E_f A_f}{f_c^{0.6} L_{failure}}} \quad (6)$$

308

309 where the reduction factor β_e accounts for the effect of edge distance a_e of concrete block
 310 on the bond strength [65]; γ_s is the height-to-width ratio of the failure contour [21] where
 311 the height of contour is equal to CFRP strip height $h_f + 1$ mm and the width is equal to the
 312 CFRP strip thickness $t_f + 2$ mm; f_c is the cylinder compressive strength of concrete; E_f
 313 is the elastic modulus of CFRP strip, A_f is the cross-sectional area of the CFRP strip;
 314 $L_{failure} = 2h_f + t_f + 4$ mm is the length of the failure contour; c_a is the smallest distance
 315 between the CFRP strip and the surface of the concrete [7]; reduction factor $\beta_{L,s}$ accounts
 316 for the bond length of CFRP strip L_b on the bond strength; and $L_{e,s}$ is the effective bond
 317 length.

318

319 *Oehlers et al.'s model [23]*

320 Based on the model by Seracino and co-workers (Eq. 2), Oehlers et al. [23] proposed a bond
 321 strength model for NSM FRP-to-concrete bonded joints containing several NSM CFRP
 322 strips:

$$P_{u,o} = \alpha_p 0.85 \beta_e \beta_{L,s} \gamma_s^{0.25} f_c^{0.33} L_{failure} \sqrt{n_f E_f A_f + k_{EAC} E_c A_c} \quad (7)$$

$$324 \quad k_{EAC} = 0.45 - 0.03(M_u/M_{cr}) \quad (8)$$

325 where n is the number of NSM FRP strips, E_c is the elastic modulus of concrete, A_c is the
 326 cross-sectional area encompassed by the failure plane, k_{EAC} is a reduction factor for axial
 327 rigidity of concrete, M_u is the applied moment at IC debonding (equal to zero for NSM
 328 FRP-to-concrete bonded joint), and M_{cr} is the moment at the initial cracking of the beam.

329

330 *Zhang et al.'s model [27]*

331 Zhang et al. [27] proposed another bond strength model, as expressed in Eq. 9. In this model,
 332 the effective bond length and the reduction factor accounting for the detrimental effect of an
 333 insufficient bond length were developed based on the bond-slip model proposed by Zhang et
 334 al. [26].

$$335 \quad P_{u,z} = \beta_{L,z} \sqrt{2G_f E_f A_f C_{failure}} \quad (9)$$

$$336 \quad G_f = 0.40 \gamma^{0.422} f_c^{0.619} \quad (10)$$

$$337 \quad L_{e,z} = \frac{1.66}{\eta} \quad \text{where} \quad \eta^2 = \frac{\tau_{max}^2 C_{failure}}{2G_f E_f A_f} \quad (11)$$

$$338 \quad \beta_{L,z} = \frac{L_b}{L_{e,z}} (2.08 - 1.08 \frac{L_b}{L_{e,z}}) \quad \text{when } L_b < L_{e,z} \quad \text{and} \quad \beta_{L,z} = 1 \quad \text{when } L_b \geq L_{e,z} \quad (12)$$

339 where L_b and $L_{e,z}$ are the bond length and effective bond length respectively; G_f is the
 340 interfacial fracture energy between NSM CFRP strip and concrete; the cross-sectional
 341 contour of the failure surface $C_{failure}$ is equal to the sum of the three side lengths of the
 342 groove; and the reduction factor $\beta_{L,z}$ accounts for the detrimental effect of insufficient bond
 343 lengths on the bond strength.

344

345 *Bilotta et al.'s model [20]*

346 More recently, Bilotta et al. [20] proposed a bond strength model based on the regression of
 347 test results collected by them. This bond strength model is originally expressed in terms of
 348 maximum strain ε_{\max} in the FRP (Eq. 13).

$$349 \quad \varepsilon_{\max} = 157 \frac{(C_{\text{failure}})^{0.66}}{(E_f A_f)^{0.823}} \quad (13)$$

350 The bond strength in terms of ultimate load can thus be obtained by multiplying Eq. 13 with
 351 $E_f A_f$:

$$352 \quad P_{u,b} = E_f A_f \varepsilon_{\max} = 157 (C_{\text{failure}})^{0.66} (E_f A_f)^{0.177} \quad (14)$$

353

354 ***Discussion on bond strength models and future research needs***

355 Among the above existing bond strength models, Bilotta et al.'s model [20] appears most
 356 inferior as it ignores the influence of both concrete strength and bond length on the bond
 357 strength. In Oehlers et al.'s model [23], the applied moment at IC debonding in a beam needs
 358 to be given first to calculate the reduction factor k_{EAC} , thus it is not a truly predictive model.
 359 Furthermore, the influence of bond length on the bond strength is also not considered in this
 360 model. Comparison between Seracino and co-workers' model [7, 21, 65] and Zhang et al.'s
 361 model [27], which was reported in Ref. [27] making use of results of 51 test specimens
 362 collected from existing studies, revealed that both models provide close predictions for the
 363 test results when the bond length of the CFRP strip is sufficiently long (not smaller than the
 364 effective bond length), but the model proposed by Zhang et al. [27] performs significantly
 365 better than Seracino and co-workers' model [7, 21, 65] when the bond length is insufficient
 366 (smaller than the effective bond length). This is mainly because that the effective bond length
 367 equation and the corresponding bond length reduction factor in the model proposed by Zhang
 368 et al. [27] are both based on an accurate bond-slip relationship obtained using a verified FE

369 model, while the effective bond length equation in the model by Seracino and co-workers [7,
370 21, 65] is based on an assumed linear-softening bond-slip relationship and the bond length
371 reduction factor is described using an assumed linear function.

372

373 It should be noted that the edge distance and the groove spacing have a significant effect on
374 the bond strength, and their influences have not been fully studied. In the model by Seracino
375 and co-workers [7, 21, 65], although a reduction factor accounting for the effect of edge
376 distance was included, it was based on regression of only limited test results by them [65]. In
377 Oehlers et al.'s model [23], although the involvement degree of the concrete encompassed by
378 the failure plane could be reflected by the groove spacing, the effect of the groove spacing on
379 the bond behavior of each FRP strip was still not considered. Some studies conducted by
380 Barros and co-workers [e.g. 82-86] on RC beams strengthened in shear with NSM FRP strips
381 can be referred to for considering the effect of groove spacing on the bond strength.
382 Considering that the failure modes of FRP strips NSM to concrete resemble those of adhesive
383 anchors, Barros and co-workers develop a model which relates the bond strength of NSM
384 FRP-concrete interface in shear-strengthened beams to the so-called "semiconical fracture
385 surface of concrete" surrounding the NSM strip. The NSM FRP strip is thought to be pulled
386 out when the principal tensile stress of concrete on this semiconical surface exceeds the
387 tensile strength of concrete. The method is able to consider the effect of groove spacing (i.e.,
388 the "interaction among adjacent strips" in their papers) on the bond behaviour between NSM
389 FRP strip and concrete: when the groove spacing is small, the semiconical fracture surfaces
390 of adjacent NSM FRP strips overlap with each other and thus the total efficient/envelop
391 fracture area becomes smaller than the direct summation of the semiconical fracture area of
392 each NSM FRP strip. While this method has the potential to be extended to study the effect of
393 groove spacing on the bond strength of bonded joints with multiple NSM FRP strips, future

394 research is needed to develop a large experimental database on such bonded joints for
395 verification/refinement of the method. It should be also noted that most existing studies on
396 the bond behaviour between NSM FRP and concrete were based on ambient temperature. The
397 effect of elevated temperature on the bond behaviour as well as the strengthening efficiency
398 of NSM FRP strips have not been clarified, while preliminary studies have been carried out
399 by researchers [e.g., 87-90]. Further studies are therefore needed to clarify the effects of edge
400 distance, groove spacing and elevated temperature for more accurate bond-strength models.

401 *3.1.3 IC interfacial debonding strength model*

402 Vasquez and Seracino [24] directly used the bond strength mode proposed by Seracino and
403 co-workers [7, 21, 65] (as expressed in Eq. 2) for NSM CFRP strip-to-concrete bonded joint
404 to predict the force in the NSM FRP strip at IC debonding in NSM CFRP RC beams.
405 Vasquez and Seracino [24] assessed this model (Eq. 2) using results of NSM CFRP RC
406 beams collected from existing studies and found that the prediction-to-test ratio is 0.88. This
407 conservative prediction is mainly because that in RC beams there usually exist more than one
408 major flexural cracks and the debonding force in the FRP between two adjacent cracks is
409 larger than that in one-side pull out test of the corresponding bonded joints, as has been
410 proved by Teng et al. [91] by using an analytical solution in an EB FRP-to-concrete bonded
411 joint. Although the above method cannot be much criticized considering that this bond
412 strength on NSM CFRP strip-to-concrete interfaces generally offers a lower bound to the IC
413 interfacial debonding strength of RC beams (thus provide a conservative prediction for design
414 purpose), a more accurate design model which can take into count the influence of
415 multi-cracks still needs to be pursued.

416

417 It can be expected that the bond strength model proposed by Zhang et al. [27] provides
418 similar prediction of IC debonding strength to that by Seracino and co-workers [7, 21, 65], in

419 the sense that in RC beams the bond length of FRP is normally larger than the effective bond
420 length. The difference between the bond strength model by Zhang et al. [27] and that by
421 Seracino and co-workers [7, 21, 65] may only be reflected in situations where the bond length
422 of NSM FRP is limited, such as in the shear strengthening of RC beams.

423 **3.2 IC Cover separation**

424 The failure process and mechanism of IC cover separation is as follows: the transfer of the
425 tensile stress from the cracked concrete onto the tension steel bars after the formation of a
426 dominating flexural crack incurs high local interfacial shear stresses near the intersection of
427 tension steel bars and the dominating flexural crack. Besides, as the steel bars are usually not
428 smooth but have some ribs on it, the relative displacement between steel bars and concrete
429 also incurs radial stresses onto the surrounding concrete as shown in Fig. 5. These high local
430 interfacial shear stresses and radial stresses increase with the applied load and finally induce
431 separation failure on the plane of the tension steel bars. Due to their different failure
432 mechanisms, the bond strength of NSM CFRP strip-to-concrete interfaces cannot be used in
433 predicting the strength of IC cover separation in NSM CFRP RC beams.

434

435 By far, although IC cover separation failure has been observed in experimental tests, it has
436 not yet attracted enough research attention. There has been no established strength model for
437 IC cover separation failure, probably because its failure mechanism is relatively complicated.
438 As mentioned earlier, the failure happens on the horizontal plane of tension steel bars, and at
439 this failure plane, the clear concrete width is smaller than the beam width because of the
440 existence of the steel bars. In addition, radial stresses exerted by the steel tension bars to the
441 surrounding concrete when the slip between the concrete and the steel tension bar develop
442 have found to further weaken the critical plane [30, 31]. An FE model taking into account the
443 above effects has been developed for establishing strength models for end cover separation in

444 EB/NSM FRP-strengthened RC beams [31] but has not yet been extended to study IC cover
445 separation. Further studies are needed to develop strength models for IC cover separation.

446

447 **4 End debonding**

448 End debonding failure mode also contains two sub-types: end interfacial debonding and end
449 cover separation. Similar to IC debonding, these two sub-types of failure were controlled by
450 different failure mechanisms and should be treated separately. Although more and more
451 attentions have been drawn to the development of end debonding strength models in NSM
452 CFRP RC beams, the existing models have been still relatively limited.

453 **4.1 End Interfacial Debonding**

454 *4.1.1 Failure mechanism*

455 When the FRP-strengthened beam is under loading, high interfacial shear and normal stresses
456 develop near the end of NSM CFRP strip as a result of the abrupt termination of the strip [e.g.
457 25, 29]. Due to the high interfacial stresses, an inclined crack usually occurs near the end of
458 the NSM FRP, and another flexural-shear crack usually appears in the bonded region of FRP
459 at a certain distance (i.e. the crack spacing) as shown in Fig. 3a. These interfacial stresses
460 increase with the applied load and finally induce the debonding between FRP and concrete.

461 *4.1.2 Strength models*

462 Two strength models have been established for end interfacial debonding failure. The first
463 one is proposed by Hassan and Rizkalla [42] based on interfacial stresses between NSM
464 CFRP strip and concrete, and the other one is originally proposed by Oehlers et al. [92, 93]
465 for FRP-plated RC beams and modified by Vasquez and Seracino [24] for NSM CFRP RC
466 beams. It should be noted that existing strength models of end debonding for FRP-plated RC
467 beams are generally not applicable to NSM CFRP RC beams, because some parameters in

468 these models were calibrated using test results of FRP-plated RC beams [94]. The two
 469 existing strength models are introduced in details here followed by a discussion of these two
 470 models.

471

472 ***Hassan and Rizkalla's model [42]***

473 For end interfacial debonding failure, Hassan and Rizkalla [42] proposed an approach for
 474 predicting the strength of NSM CFRP RC beams. Based on the interfacial stress analysis of
 475 Malek et al. [95] for EB FRP systems, Hassan and Rizkalla [42] gave closed-form
 476 expressions to predict the interfacial shear stress τ between NSM CFRP strip and concrete,
 477 as expressed in Eqs. 15 and 16 respectively for a simply-supported beam subjected to a point
 478 load and a simply-supported beam subjected to two symmetric point loads:

$$479 \quad \tau = \frac{t_f}{2} \left[\frac{n_f P a y_{eff}}{2I_{eff}} \omega e^{-\omega x} + \frac{n_f P y_{eff}}{2I_{eff}} \right] \quad (15)$$

$$480 \quad \tau = \frac{t_f}{2} \left[\frac{n_f P y_{eff}}{I_{eff}} + \frac{n_f P y_{eff} a}{I_{eff}} \omega e^{-\omega x} \right] \quad (16)$$

$$481 \quad \omega^2 = \frac{2G_a}{t_a t_f E_f} \quad (17)$$

482 where x is the horizontal distance from the strip end, t_f is the thickness of the CFRP strip,

483 $n_f = \frac{E_f}{E_c}$ is the modulus ratio between FRP and concrete, P is the point load, y_{eff} is the

484 distance from the strip centroid to the neutral axis of the section, a is the distance from the
 485 strip end to the nearest support; I_{eff} is the effective moment of inertia and is expressed in Eq.

486 18, e is the base of the natural logarithm, and G_a and t_a are the shear modulus and
 487 thickness of the adhesive respectively,

$$I_{eff} = \left(\frac{M_{cr}}{M_a} \right)^3 I_g + \left(1 - \left(\frac{M_{cr}}{M_a} \right)^3 \right) I_{cr} \quad (18)$$

where M_{cr} and M_a are the cracking and applied moments on a beam section respectively, I_g is the transformed gross moment of inertia in terms of concrete of the strengthened section, and I_{cr} is the transformed moment of inertia in terms of concrete of the cracked section.

Obviously, the interfacial stresses obtained from Eqs. 15 and 16 peak when $x = 0$, indicating that the cut-off point is the critical location for the initiation of debonding failure. By introducing the Mohr-Coulomb failure criterion, the interfacial stress τ_{max} at failure can be expressed as

$$\tau_{max} = \frac{f_c f_t}{f_c + f_t} \quad (19)$$

where f_c and f_t are the cylinder compressive strength and tensile strength of concrete respectively.

Substituting Eq. 19 into Eq. 15 or Eq. 16 with $x=0$ yields the applied load at end debonding failure of the strengthened beam.

Oehlers et al.'s model [92, 93]

Oehlers et al. [92, 93] referred to end debonding failures with the end of the EB FRP plate located in the shear span as the Critical Diagonal Crack (CDC) debonding. Based on Zhang's method [96] for determining the shear strength of RC beams, Oehlers et al. [92, 93] proposed a "passive prestress model" of CDC debonding for simply supported beams under

510 concentrated loads. In this approach, two shear forces are considered: the shear force V_{crack}
 511 causing the diagonal crack (Eq. 20) and the shear force V_{slide} causing the sliding of the
 512 diagonal crack (Eq. 21). CDC debonding failure is assumed to occur when these two shear
 513 forces become equal to each other.

$$514 \quad V_{crack} a_v = (x_d^2 + h^2) \left(\frac{b f_{tef}}{2} + \frac{f_t n_f A_f}{h} \right) + F_{ps} h_{ps} \quad (20)$$

$$515 \quad V_{slide} = 0.4 f_c b h \left(1 + 2 \frac{F_{ps} + P_{axial}}{f_c b h} \right) \left(\sqrt{1 + \left(\frac{x_d}{h} \right)^2} - \frac{x_d}{h} \right) f_1 f_2 f_3 \quad (21)$$

$$516 \quad f_1 = \frac{3.5}{\sqrt{f_c}} \quad (22)$$

$$517 \quad f_2 = 0.27 \left(1 + \frac{31.6}{\sqrt{h}} \right) \quad (23)$$

$$518 \quad f_3 = 15 \frac{A_s}{b h_0} + 0.58 \quad (24)$$

519 where $f_{tef} = 0.156 (f_c)^{2/3} \left(\frac{h}{100} \right)^{-0.3}$ and f_t are the the effective tensile strength and tensile
 520 strength of concrete respectively, a_v is the shear span of the beam, x_d is the horizontal
 521 distance between the bottom position of the diagonal crack and the applied concentrated load,
 522 h is the beam height, A_f is the cross-sectional area of FRP, P_{axial} is the maximum axial
 523 force in the FRP, F_{ps} is the tendon prestressing force, h_{ps} is the depth of the tendon
 524 prestressing force position, and f_1 , f_2 and f_3 are functions of concrete strength, beam
 525 height and tension reinforcement ratio respectively.

526

527 For FRP-plated RC beams, the value of P_{axial} can be calculated using the bond strength
 528 model proposed by Chen and Teng [78], as recommended by Oehlers et al. [92, 93]. To make

529 this model applicable to NSM CFRP RC beams, Vasquez and Seracino [24] recommended
530 that the value of P_{axial} can be predicted by the bond strength model proposed by Seracino et
531 al. [21] for NSM CFRP strip-to-concrete interface.

532 *4.1.3 Discussions and future research needs*

533 Hassan and Rizkalla' model [42] offered a valuable pioneering study on end debonding
534 strength models in RC beams strengthened with NSM CFRP strips. In this model, however,
535 only the longitudinal shear stress is taken into account to determine whether debonding
536 failure occurs, which to some extent lacks rigor. Vasquez and Seracino [24] assessed this
537 model and found that the model was significantly conservative. This implies that the local
538 failure in the concrete layer at the end of the FRP strip does not mean the debonding failure
539 of the beam. As indicated by Vasquez and Seracino [24], Oehlers et al.'s model [92, 93] may
540 be overly conservative, because the contribution of stirrups was not taken into account. The
541 omission of the contribution of stirrups may be acceptable for FRP-plated RC beams but not
542 reasonable for NSM CFRP RC beams. This is because that the debonding strain in the NSM
543 FRP strip is usually larger than that in EB FRP plate, thus a higher strain in stirrup can be
544 possibly developed. A comparison made by Vasquez and Seracino [24] showed that Oehlers
545 et al.'s model [92, 93] gave an average prediction-to-test ratio of 0.74 for the collected
546 specimens.

547
548 Obviously, the existing strength models for end interfacial debonding are quite limited. The
549 interfacial stress based model [42] usually underestimates the debonding strength of the beam.
550 The local failure in the concrete at the end of NSM CFRP strip cannot be treated as the
551 debonding failure of the strengthened RC beam, as cracks on the tension surface of the beam
552 makes interfacial stress redistribute before debonding failure. The prestress beam model [92,
553 93] ignores the contribution of the stirrups, which is not reasonable in RC beams

554 strengthened with NSM CFRP strips. In fact, the “concrete tooth model”, which has been
555 used in the establishment of end debonding strength models in steel/FRP-plated RC beams
556 [e.g. 97, 98], is worth studying as the description of the failure mechanism is clear and is
557 similar to the observation in tests. Unfortunately, however, no such attempt has been carried
558 out in establishing strength models of end interfacial debonding in RC beams strengthened
559 with NSM CFRP strips.

560 **4.2 End cover separation**

561 *4.2.1 Failure mechanism*

562 Similar to end interfacial debonding, due to high interfacial stresses developed near the end
563 of NSM FRP strips [e.g. 25, 29], an inclined crack first occurs near the end of the NSM FRP,
564 and then another flexural-shear crack appears in the bonded region of FRP at a certain
565 distance (i.e. the crack spacing) as shown in Fig. 3b. When these cracks further develop and
566 intersect with the steel tension bars, the concrete cover between the two cracks forms a “tooth”
567 whose top is dragged by the NSM CFRP strip in the shear direction. The concrete near the
568 intersection of the tension steel bar and the inclined crack near the end of the NSM FRP
569 (Point A in Fig. 3b) is subjected to a combined effect of the following aspects: (1) the tensile
570 stress induced by the bending moment as a result of the drag force on the top of the “tooth”;
571 (2) the shear stress induced by the drag force on the top of the “tooth”; (3) the clear concrete
572 width is smaller than the beam due to the existence of the steel bars; and (4) more importantly,
573 radial stresses (as shown in Fig. 5) may be generated by the steel tension bars onto the
574 surrounding concrete when slips between the concrete and the steel occur. Therefore, the
575 plane of the tension steel bars becomes the critical plane and a major crack forms on this
576 plane when the tensile and shear stress on this place reaches a critical level. This major crack
577 travels along the steel bar from the end of the NSM CFRP strip to mid-span of the beam as
578 the applied load goes up, as shown in Fig. 3b.

579 4.2.2 Strength models

580 By far, two strength models of end cover separation have been respectively proposed by De
 581 Lorenzis and Nanni [99] and Al-Mahmoud et al. [9] for NSM round FRP bar-strengthened
 582 RC beams, based on the “concrete tooth” concept, in which, the concrete cover between two
 583 adjacent cracks was treated as a concrete tooth (cantilever) under the horizontal shear force
 584 exerted by the attached FRP. These two models can be also applied to NSM FRP
 585 strip-strengthened RC beams with proper modifications. More recently, Teng et al. [28]
 586 developed a strength model for end cover separation in NSM FRP strip-strengthened RC
 587 beams, also based on the “concrete tooth” concept. These three strength models are described
 588 here followed by a discussion of their performance.

589

590 ***De Lorenzis and Nanni’s model [99]***

591 De Lorenzis and Nanni [99] extended the strength model proposed by Zhang et al. [97] and
 592 Raouf and Zhang [100] to calculate the strength of RC beams strengthened with NSM round
 593 FRP bars at end cover separation. This model was the first attempt to expose end cover
 594 separation strength model for NSM FRP-strengthened RC beams and is based on the concept
 595 of the concept of “concrete tooth”. By assuming a linear elastic behaviour, the normal stress
 596 σ_A at the tension corner near the root of the concrete tooth (i.e. Point A in Fig. 3b which is
 597 near the intersection of the tension steel bar and the inclined crack near the end of the NSM
 598 FRP) could be calculated as

$$599 \quad \sigma_A = \frac{M_A}{I_A} \left(\frac{l}{2} \right) \quad (25)$$

600 where $M_A = n\pi d_b l h'$ is the bending moment at the root of the concrete tooth, $I_A = bl^3/12$

601 is the sectional moment of inertia of the concrete tooth, l is the minimum crack spacing

602 l_{\min} or maximum crack spacing $l_{\max} = 2l_{\min}$, h' is the vertical distance from the root of the

603 concrete tooth to the centroid of NSM FRP, b is the beam width, d_b and n are the
 604 diameter and number of the FRP round bars respectively, and τ is the shear bond stress
 605 between NSM FRP bar and concrete. By assuming that failure of the beam occurs when the
 606 stress σ_A is equal to the tensile strength of concrete f_t , the shear bond stress $\tau_{failure}$ at
 607 failure can be expressed as

$$608 \quad \tau_{failure} = \frac{f_t l}{6h} \frac{b}{n\pi d_b} \quad (26)$$

609 The shear stress should be equilibrated by the FRP axial stress. At the critical section (such as
 610 the section corresponding to the loading points), the critical FRP axial stress can be
 611 calculated as

$$612 \quad \sigma_{failure} = \frac{4\tau_{failure} L_p}{d_b} \quad (27)$$

613 where L_p is the effective length of the NSM FRP bar in the shear span within which the
 614 interfacial stress is assumed to be uniformly distributed. The value of L_p was determined by
 615 these authors to be the smaller one of L_{p1} and L_{p2} , where L_{p1} is the length of the NSM
 616 FRP bar in the shear span and L_{p2} is the equivalent length given by

$$617 \quad L_{p2} = \begin{cases} 1.86l_{min}^2 - 127l_{min} + 2436 & \text{if } l_{min} \leq 50mm \\ 736 & \text{if } l_{min} > 50mm \end{cases} \quad (28)$$

618 where the minimum crack spacing l_{min} can be calculated as

$$619 \quad l_{min} = \frac{A_e f_t}{u_s \sum O_s + u_f \sum O_f} \quad (29)$$

620 where A_e is the area of concrete in tension and is assumed to be product of the beam width
 621 and twice of the distance from the centroid of steel tension bars to the soffit of the beam,

622 $f_t = 0.36\sqrt{f_{cu}}$ is the tensile strength of concrete, f_{cu} is the cube compressive strength of

623 concrete, $\sum O_s$ is the total perimeter of the steel tension bars, $\sum O_f$ is the total perimeter of
 624 the NSM FRP round bars, $u_s = 0.28\sqrt{f_{cu}}$ is the average local bond strength between steel
 625 bars and concrete, and u_f is the average bond strength between NSM FRP bars and concrete
 626 and was recommended by De Lorenzis and Nanni [99] to be the local bond strength.

627

628 In order to apply the above model to NSM CFRP RC beams, the following modifications
 629 need to be made: (1) the bending moment M_A at the root of the concrete tooth should be
 630 calculated based on the geometry of NSM CFRP strips; (2) the effective length L_p should
 631 be recalibrated using test results of NSM CFRP strip-strengthened RC beams ; and (3) the
 632 average bond strength between NSM FRP bars and concrete u_f should be calibrated using
 633 bond strength model of NSM CFRP strip-to-concrete interface.

634

635 *Al-Mahmoud et al.'s model [9]*

636 The model proposed by Al-Mahmoud et al. [9] is quite similar to that proposed by De
 637 Lorenzis and Nanni [99]. In this model, the bending moment M_A at the root of the concrete
 638 tooth is related to the FRP axial stress at the left cracked section (if the FRP is terminated on
 639 the right) as

$$640 \quad M_A = \sigma_f A_f h' \quad (30)$$

641 The axial stresses in the FRP at the left cracked section can therefore be calculated as

$$642 \quad \sigma_f = \frac{M_A}{A_f h'} = \frac{bl^2}{6A_f d_b} \quad (31)$$

643 σ_f can also be expressed in terms of the bending moment M_l of the strengthened beam at
 644 the left cracked section as

$$\sigma_f = n_f \left(\frac{d_f - y_0}{I_{cr}} \right) M_l \quad (32)$$

645 With the assumption that the end cover separation happens as the tensile stress in the concrete
 646 at the tension corner near the root of the concrete tooth (i.e. Point A in Fig. 3b), combining
 647 Eqs. 31 and 32 gives the following equation for calculating the bending moment of the
 648 strengthened beam at the left cracked section at debonding failure:
 649

$$M_l = \frac{f_t I_{cr} b l^2}{6 n_f A_f d_b (d_f - y_0)} \quad (33)$$

651 Where I_{cr} is the transformed moment of inertia in terms of concrete of the cracked section,
 652 d_f is the vertical distance from the centroid of the NSM FRP to the top surface (in
 653 compression) of the beam, and y_0 is the vertical distance from the neutral axis of the
 654 cracked section to the top surface of the beam.

655 ***Teng et al.'s model [28]***

656 The model developed by Teng et al. [28] to predict the end cover separation strength of NSM
 657 CFRP RC beams is based on the following idea: if the FRP strain on the left crack section
 658 (Point B in Fig. 6) at end cover separation failure is known, the bending moment on the
 659 corresponding section can be obtained through a section analysis, and the ultimate load can
 660 then be easily calculated by dividing the bending moment by the horizontal distance from the
 661 left crack section to the nearest support. To obtain the strain in the FRP at the left cracked
 662 section at failure (Point B in Fig. 6), the simplified FE model proposed by Zhang and Teng
 663 [32] was adopted in Teng et al. [28]. In this FE model, the part of the RC beam between the
 664 two cracks near the FRP end was isolated from the beam (Fig. 6), the bending moments
 665 acting on the two cracked sections was realized through the external loads as shown in Fig. 6,
 666 and the plane section assumption was achieved using a rigid plate attached to each cracked

668 section. Furthermore, the radial stresses exerted by the tension steel bars onto the surrounding
 669 concrete were modelled using a proposed cohesive-element-pair (CEP). The plane section
 670 assumption may not be exactly valid here, but it can simplify the FE model and may not
 671 introduce substantial errors. An equation for the FRP strain at the left cracked section at end
 672 cover separation failure was then developed through the regression of results of a numerical
 673 parametric study using the abovementioned simplified FE model:

$$674 \quad \varepsilon_{db} = 10^4 \times \beta_{cs} \beta_{AE} \beta_{bod} b_{clear} \sqrt{f_c} \quad (34)$$

$$675 \quad \beta_{cs} = \left(\frac{4.5}{s_c^{0.3}} - \frac{c}{s_c} \right) \left(\frac{s_c}{100} - 0.1 \right) \quad (35)$$

$$676 \quad \beta_{AE} = \frac{1}{(A_f E_f)^{0.9}} \quad (36)$$

$$677 \quad \beta_{bod} = \left(\frac{b_{clear}}{D_t} \right)^{0.1} \quad (37)$$

678 where β_{cs} is a factor accounting for the combined effect of s_c (crack spacing, in mm) and
 679 c_d (distance from the centroid of steel bars to that of FRP reinforcements, in mm) on the
 680 failure strain; β_{AE} is a factor accounting for the effect of axial stiffness of FRP strip $A_f E_f$
 681 (A_f in mm^2 and E_f in GPa); and β_{bod} is a factor accounting for the effect of ratio
 682 between the clear concrete width b_{clear} (in mm) and the sum of steel tension bar diameters
 683 D_t (in mm). The cylinder compressive strength of concrete f_c is given in MPa .

684
 685 The value of the cracking spacing influences the FRP strain at the left cracked section at
 686 failure and the distance from the left cracked section to the nearest support. In Teng et al.'s
 687 model [28], the adopted model for minimum crack spacing s_c^{\min} is also the one proposed by
 688 Zhang et al. [97], as expressed in Eq. 29 with $u_f = 0.28\sqrt{f_{cu}}$. According to Zhang et al. [97],

689 the possible crack spacing value should be in the range from s_c^{\min} to $2s_c^{\min}$.

690 4.2.3 Discussions and future research needs

691 As De Lorenzis and Nanni's model [99] was originally proposed for NSM FRP round
692 bar-strengthened RC beams, modifications should be made first to satisfy the geometric and
693 mechanical properties of NSM CFRP strips. By now, however, the effective length L_p and
694 the average bond strength u_f have not been calibrated by the authors or other researchers
695 using test results of NSM FRP strip-strengthened RC beams, thus it cannot yet be used for
696 predicting the cover separation strength in such FRP-strengthened RC beams. Both De
697 Lorenzis and Nanni's model [99] and Al-Mahmoud et al. 's model [9] only took account for
698 the tensile stress induced by the bending moment as a result of the drag force on the top of
699 the "tooth" but not the shear stress induced at the same time. Furthermore, the weakness of
700 the beam by the tension steel bars and the radial stresses were not considered in these two
701 strength models. Teng et al.'s model [28] was based on results of the parametric study using
702 an FE model which reflected all the above mentioned influencing factors. The performance of
703 Teng et al.'s model [28], however, is significantly influenced by the accuracy of the model of
704 crack spacing which is usually in a range from s_c^{\min} to $2s_c^{\min}$. Teng et al. [28] compared the
705 predictions of their model with collected test specimens, with the crack spacing being the
706 minimum stabilized value s_c^{\min} , the maximum stabilized value $2s_c^{\min}$, and an intermediate
707 value $1.5s_c^{\min}$ respectively to examine the effect of crack spacing. It was found that the
708 predictions of Teng et al.'s model [28] with crack spacings of $1.5s_c^{\min}$ and $2s_c^{\min}$ led to
709 average prediction-to-test ratios of 1.10 and 1.17 respectively; their standard deviations
710 (STDs) were 0.119 and 0.172 and their coefficient of variations (CoVs) were 0.108 and 0.147
711 respectively. These statistics were much better than predictions of Teng et al.'s model [28]
712 obtained with a crack spacing of s_c^{\min} whose average prediction-to-test ratio, STD and CoV

713 are 0.863, 0.155 and 0.180 respectively. Nevertheless, the model by Teng et al. [28] with any
714 of the above three values of crack spacing offered much closer predictions to the test results
715 than the model Al-Mahmoud et al. [9], the predictions of which were un-conservative, with
716 the average prediction-to-test ratio, STD and CoV being 1.90, 1.34 and 0.702 respectively.

717

718 ***4.3 Anchorage Measures for Preventing End Debonding***

719 In design, if debonding cannot be eliminated, IC debonding is preferable to end debonding
720 because the latter usually happens in a brittle manner without any noticeable early warning.
721 By now, metallic and non-metallic anchorage measures have been investigated in
722 experimental tests for preventing/mitigating end debonding in RC beams strengthened in
723 flexure with an EB FRP/steel plate. The metallic anchorage measures, in the form of steel
724 bolts, steel clamps or steel U-jackets, were initially proposed for preventing end debonding in
725 steel-plated RC beams [e.g. 101, 102]. The metallic anchorage measures, however, suffer
726 from the following two disadvantages: the difficulty of installation and the poor resistance to
727 corrosion. Therefore, non-metallic anchorage measures (such as FRP-based anchorage
728 measures) are more attractive than metallic anchorage measures in FRP-strengthened RC
729 beams for preventing end debonding. A number of studies have been conducted to explore
730 the effectiveness of FRP U-jackets in preventing/mitigating end debonding failure in
731 FRP-plated RC beams [e.g. 103-108], while the studies on the use of FRP U-jackets as
732 anchorage measures for NSM FRP bars in NSM FRP-strengthened RC beams have been
733 rather limited. These limited existing studies, however, have revealed that FRP U-jackets are
734 quite effective in both postponing the end debonding of the beam and enhancing the ductility
735 of the beam [50, 57, 109]. Before a reliable and economical design procedure for FRP
736 U-jackets can be established for confident use in practice, future research should be
737 conducted to address the following issues: (1) more experimental studies on the use of FRP

738 U-jackets as the end anchorage measure of NSM FRP reinforcement should be conducted to
739 provide a larger database; (2) the effect of the angle of FRP U-jackets inclined with respect to
740 the beam axis on the effectiveness of preventing end debonding in NSM FRP-strengthened
741 RC beams needs to be clarified; (3) the effect of termination position of NSM FRP
742 reinforcement (resulting in different section moment-shear force combination at the FRP end)
743 on the performance of FRP U-jackets in preventing/mitigating end debonding failure in NSM
744 FRP-strengthened RC beams needs to be studied; and (4) reliable FE approaches need to be
745 established for a reliable design procedure for FRP U-jackets as end anchorage measures.

746

747 **5 Concluding remarks**

748 This paper has presented a critical review of the existing knowledge on NSM CFRP strips for
749 flexural strengthening of RC beams. This review has been focused on the debonding failure
750 modes in such FRP-strengthened RC beams, the mechanisms behind, and the corresponding
751 strength models. The following conclusions can be made from the review:

752

- 753 1) The NSM FRP strengthening method is much more efficient than the EB FRP method in
754 the flexural strengthening of RC beams, and NSM CFRP strips are superior to NSM FRP
755 bars of other sectional forms (such as round bars and square bars) due to a larger
756 perimeter-to-sectional-area-ratio of the former;
- 757 2) The desired debonding failure mode at the NSM FRP-to-concrete interface is the
758 cohesion failure in a thin layer of concrete near the adhesive-to-concrete interface. This
759 failure model can be achieved if the surfaces of concrete and CFRP are appropriately
760 treated and a proper adhesive is used;

- 761 3) Several local bond-slip models and bond strength models have been proposed for NSM
762 CFRP strips-to-concrete interfaces. Some of them can now provide accurate predictions
763 for single NSM FRP strip-to-concrete joints with sufficient concrete edge distances;
- 764 4) A number of experimental studies have been conducted on NSM CFRP RC beams,
765 which have led to the identification of four debonding failure modes. Concrete cover
766 separation has been found to be more often than interfacial debonding in NSM CFRP RC
767 beams.

768

769 The review presented in this paper also suggests that the existing research is still very limited
770 and the major gaps which need to be addressed by future research include:

771

- 772 1) There is a lack of experimental tests with sophisticated instrumentation which is
773 necessary to thoroughly demonstrate the validity the existing bond-slip models for NSM
774 CFRP strip-to-concrete bonded joints;
- 775 2) There is a lack of understanding on the effect of the concrete edge distance, the groove
776 spacing and elevated temperature on the bond behaviour of NSM FRP-to-concrete joints;
- 777 3) Most experimental studies were focused on simply supported RC beams where NSM
778 FRP reinforcement was applied in a sagging moment region, while little research has
779 been carried out on the use of NSM FRP reinforcement in hogging moment regions (e.g.
780 in RC frames). In the latter case, future research is needed to clarify the possible
781 difference in the strengthening mechanism, especially in terms of the anchorage failure
782 of the NSM reinforcement;
- 783 4) Only a limited number of strength models were proposed for IC interfacial debonding,
784 end interfacial debonding and end cover separation in NSM CFRP RC beams, while no
785 strength model has been established for IC cover separation. Most existing strength

786 models for NSM CFRP RC beams are preliminary in nature and have been based on
787 limited understanding of failure mechanisms. Although Teng et al.'s model [28] for end
788 cover separation, proposed based on a comprehensive numerical parametric study,
789 captures the failure mechanism of such failure mode, the accuracy of this model needs to
790 be further verified with more test data;

791 5) Using U-shaped FRP jackets for end anchorage of NSM CFRP strips was shown to
792 enhance the strengthening efficiency. However, its effect has not been quantitatively
793 investigated and no design method is available now.

794

795 **6 Acknowledgement**

796 The authors are grateful for the financial support received from the National Natural Science
797 Foundation of China (Project Nos. 51108097, 51378130), and the Australian Research
798 Council through a Discovery Early Career Researcher Award (Project ID: DE140101349) for
799 the second author. The work presented in this paper was undertaken under the supervision of
800 Prof. Jin-Guang Teng from The Hong Kong Polytechnic University. The authors are grateful
801 to Prof. Teng for his contributions to this work.

802

803 **References:**

- 804 [1] Teng, J. G., Chen, J. F., Smith, S. T., and Lam, L. (2002). *FRP-strengthened RC*
805 *Structures*, West Sussex: Wiley.
- 806 [2] Hollaway, L. C. and Teng, J. G., eds. (2008). *Strengthening and rehabilitation of civil*
807 *infrastructures using FRP composites*, Woodhead, Cambridge, U.K.
- 808 [3] El Hacha, R., and Rizkalla, S. H. (2004). "Near-surface-mounted fiber-reinforced
809 polymer reinforcements for flexural strengthening of concrete structures." *ACI*
810 *Structural Journal*, 101(5), 717-726.
- 811 [4] De Lorenzis, L., and Teng, J. G. (2007). "Near-surface mounted FRP reinforcement: an
812 emerging technique for strengthening structures." *Composites Part B-Engineering*,
813 38(2), 119-143.
- 814 [5] Coelho, M.R.F., Sena-Cruz, J.M., Neves, L.A.C. (2015). "A review on the bond
815 behavior of FRP NSM systems in concrete." *Construction and Building Materials*, 93,
816 1157-1169.

- 817 [6] Seracino, R., Jones, N. M., Ali, M. S. M., Page, M. W., and Oehlers, D. J. (2007).
818 “Bond strength of near-surface mounted FRP strip-to-concrete joints.” *Journal of*
819 *Composites for Construction*, 11(4), 401-409.
- 820 [7] Oehlers, D. J., Haskett, M., Wu, C. Q., and Seracino, R. (2008). “Embedding NSM FRP
821 plates for improved IC debonding resistance.” *Journal of Composites for Construction*,
822 12(6), 635-642.
- 823 [8] Al-Mahmoud, F., Castel, A., Francois, R., and Tourneur, C. (2009). “Strengthening of
824 RC members with near-surface mounted CFRP rods.” *Composite Structures*, 91(2),
825 138-147.
- 826 [9] Al-Mahmoud, F., Castel, A., Francois, R., and Tourneur, C. (2010). “RC beams
827 strengthened with NSM CFRP rods and modelling of peeling-off failure.” *Composite*
828 *Structures*, 92(8), 1920-1930.
- 829 [10] Wang, B., Teng, J. G., De Lorenzis, L., Zhou, L. M., Ou, J. P., Jin, W., and Lau, K. T.
830 (2009). “Strain monitoring of RC beams strengthened with smart NSM FRP bars.”
831 *Construction and Building Materials (Special Issue)*, 23(4), 1698-1711.
- 832 [11] Ceroni, F. (2010). “Experimental performances of RC beams strengthened with FRP
833 materials.” *Construction and Building Materials*, 24(9), 1547-1559.
- 834 [12] Soliman, S. M., El-Salakawy, E., and Benmokrane, B. (2010). “Flexural behaviour of
835 concrete beams strengthened with near surface mounted fibre reinforced polymer bars.”
836 *Canadian Journal of Civil Engineering*, 37(10), 1371-1382.
- 837 [13] Wahab, N., Soudki, K. A., and Topper, T. (2010). “Mechanism of bond behavior of
838 concrete beams strengthened with near-surface-mounted CFRP rods.” *Journal of*
839 *Composites for Construction*, 15(1), 85-92.
- 840 [14] Ceroni, F., Pecce, M., Bilotta, A., and Nigro, E. (2012). “Bond behavior of FRP NSM
841 systems in concrete elements.” *Composites Part B-Engineering*, 43(2), 99-109.
- 842 [15] Ceroni, F., Barros, J.A.O., Pecce, M., Ianniciello, M. (2013). “Assessment of nonlinear
843 bond laws for near-surface-mounted systems in concrete elements.” *Composites Part*
844 *b-Engineering*, 45 (1), 666-681.
- 845 [16] Lee, D., Cheng, L.J., Hui, J.Y.G. (2013). “Bond characteristics of various NSM FRP
846 reinforcements in concrete.” *Journal of Composites for Construction-ASCE*, 17(1),
847 117-129.
- 848 [17] Seo, S.Y., Feo, L. and Hui D. (2013). “Bond strength of near surface-mounted FRP
849 plate for retrofit of concrete structures.” *Composite Structures*, 95, 719-727.
- 850 [18] Bilotta, A., Ceroni, F., Di Ludovico, M., Nigro, E., Pecce, M. and Manfredi, G. (2011).
851 “Bond Efficiency of EBR and NSM FRP Systems for Strengthening Concrete
852 Members.” *Journal of Composites for Construction-ASCE*, 15(5), 757-772.
- 853 [19] Bilotta, A., Ceroni, F., Nigro, E. and Pecce, M. (2014). “Strain assessment for the
854 design of NSM FRP systems for the strengthening of RC members.” *Construction and*
855 *Building Materials*, 69, 143-158.
- 856 [20] Bilotta, A., Ceroni, F., Nigro, E. and Pecce, M. (2015). “Efficiency of CFRP NSM
857 strips and EBR plates for flexural strengthening of RC beams and loading pattern
858 influence.” *Composite Structures*, 124, 163-175.
- 859 [21] Seracino, R., Saifulnaz, M. R. R., and OehlerS, D. J. (2007). “Generic debonding
860 resistance of EB and NSM plate-to-concrete joints.” *Journal of Composites for*
861 *Construction*, 11(1), 62-70.
- 862 [22] Ali, M.S.M., Oehlers, D.J., Seracino, M.C.G. (2008) “Interfacial stress transfer of near
863 surface mounted FRP-to-concrete joints.” *Engineering Structures*, 30(7),1861-1868.
- 864 [23] Oehlers, D. J., Rashid, R., and Seracino, R. (2008). “IC debonding resistance of groups
865 of FRP NSM strips in reinforced concrete beams.” *Construction and Building Materials*,
866 22(7), 1574-1582.

- 867 [24] Vasquez, D., and Seracino, R. (2010). "Assessment of the predictive performance of
868 existing analytical models for debonding of near-surface mounted FRP strips."
869 *Advances in Structural Engineering*, 13(2), 299-308.
- 870 [25] Zhang, S.S. and Teng, J.G. (2013). "Interaction forces in RC beams strengthened with
871 near-surface mounted rectangular Bars." *Composites Part B: Engineering*, 45(1),
872 697-709.
- 873 [26] Zhang, S.S., Teng, J.G., and Yu, T. (2013). "Bond-slip model for CFRP strips
874 near-surface mounted to concrete." *Engineering structures*, 56, 945–953.
- 875 [27] Zhang, S.S., Teng, J.G., and Yu, T. (2013). "Bond strength model for CFRP strips
876 near-surface mounted to concrete." *Journal of Composites for Construction*, ASCE, in
877 press [doi:10.1061/(ASCE)CC.1943-5614.0000402].
- 878 [28] Teng J.G., Zhang S.S. and Chen J.F. (2016). "Strength model for end cover separation
879 Failure in RC beams strengthened with near-surface mounted (NSM) FRP strips",
880 *Engineering Structures*, 110, 222–232.
- 881 [29] Zhang, S.S. and Yu T. (2016). "Analytical solution for interaction forces in beams
882 strengthened with near-surface mounted round bars", *Construction and Building*
883 *materials*, 106, 189–197.
- 884 [30] Zhang, S. S., and Teng, J. G. (2010) "Finite element prediction of plate-end cover
885 separation in FRP-strengthened RC beams." *Proceedings, 11th International*
886 *Symposium on Structural Engineering*, December 18-20, 2010, Guangzhou, China, pp.
887 1794-1799.
- 888 [31] Zhang, S.S., Teng, J.G. (2014). "Finite element analysis of end cover separation in RC
889 beams strengthened in flexure with FRP." *Engineering Structures*, 75, 550-560
- 890 [32] Zhang, S.S. and Teng, J.G. (2015). "End cover separation in RC beams strengthened in
891 flexure with bonded FRP reinforcement: simplified finite element approach", *Materials*
892 *and Structures*, in press [doi:10.1617/s11527-015-0645-z].
- 893 [33] Borchert, K., and Zilch, K. (2007). "A general bond stress-slip relationship for NSM
894 FRP strips." *Proceedings, 8th International Conference on Fibre Reinforced Plastics*
895 *for Reinforced Concrete Structures*, Patras, Greece, July 16-18, 2007 (CD-ROM).
- 896 [34] Perera, W. K. K. G., Ibell, T. J., and Darby, A. P. (2009). "Bond behaviour and
897 effectiveness of various shapes of NSM CFRP bars." *Proceedings, 9th International*
898 *Symposium on Fiber-Reinforced Polymers Reinforcement for Concrete Structures*
899 *(FRPRCS-9)*, July 13-15, 2009, Sydney, Australia (CD-ROM).
- 900 [35] Perera, W. K. K. G., Ibell, T. J., and Darby, A. P. (2013). "Bond characteristics of near
901 surface mounted CFRP bars." *Construction and Building Materials*, 43, 58-68.
- 902 [36] Teng, J.G., Smith, S., Lam, L., Dai, J.G., Yu, T., Wu, Y.F., Chen, G.M. and Zhang, S.S.
903 (2016) "Guide for the strengthening of reinforced concrete structures using FRP
904 composites". To be published by the Hong Kong Society for Composites in
905 Infrastructure.
- 906 [37] De Lorenzis, L. (2002). *Strengthening of RC Structures with Near Surface Mounted*
907 *FRP Rods*. PhD Thesis, Department of Innovation Engineering, University of Lecce,
908 Italy.
- 909 [38] De Lorenzis, L. (2004). "Anchorage length of near-surface mounted fibre-reinforced
910 polymer bars for concrete strengthening-analytical modeling." *ACI Structural Journal*,
911 101(3), 375-386.
- 912 [39] Rizkalla, S., and Hassan, T. (2002). "Effectiveness of FRP for strengthening concrete
913 bridges." *Structural Engineering International*, 12(2), 89-95.
- 914 [40] Singh, S. B., Reddy, A. L. and Khatri, C. P. (2013). "Experimental and Parametric
915 Investigation of Response of NSM CFRP-Strengthened RC Beams." *Journal of*
916 *Composites for Construction-ASCE*, in press.

- 917 [41] Capozucca, R. and Bossoletti, S. (2014). "Static and free vibration analysis of RC
918 beams with NSM CFRP rectangular rods." *Composites Part B-Engineering*, 67, 95-110.
- 919 [42] Hassan, T. K., and Rizkalla, S. H. (2003). "Investigation of bond in concrete structures
920 strengthened with near surface mounted carbon fiber reinforced polymer strips."
921 *Journal of Composites for Construction, ASCE*, 7(3), 248-257.
- 922 [43] Barros, J. A. O., and Fortes, A. S. (2005). "Flexural strengthening of concrete beams
923 with CFRP laminates bonded into slits." *Cement & Concrete Composites*, 27(4),
924 471-480.
- 925 [44] Barros, J. A. O., Dias, S. J. E., and Lima, J. L. T. (2007). "Efficacy of CFRP-based
926 techniques for the flexural and shear strengthening of concrete beams." *Cement &
927 Concrete Composites*, 29(3), 203-217.
- 928 [45] Teng, J. G., De Lorenzis, L., Wang, B., Rong, L., Wong, T. N., and Lam, L. (2006).
929 "Debonding failures of RC beams strengthened with near-surface mounted CFRP strips."
930 *Journal of Composites for Construction, ASCE*, 10(2), 92-105.
- 931 [46] Aidoo, J., Harries, K. A., and Petrou, M. F. (2006). "Full-scale experimental
932 investigation of repair of reinforced concrete interstate bridge using CFRP materials."
933 *Journal of Bridge Engineering*, 11(3), 350-358.
- 934 [47] Yost, J. R., Gross, S. P., Dinehart, D. W., and Mildenberg, J. J. (2007). "Flexural
935 behavior of concrete beams strengthened with near-surface mounted CFRP strips." *ACI
936 Structural Journal*, 104(4), 430-437.
- 937 [48] Castro, E. K., Melo, G. S., and Nagato, Y. (2007). "Flexural strengthening of RC "T"
938 beams with near surface mounted (NSM) FRP reinforcements." *Proceedings, 8th
939 International Conference on Fibre Reinforced Plastics for Reinforced Concrete
940 Structures*, Patras, Greece, July 16 to 18, 2007 (CD-ROM).
- 941 [49] Kotynia, R. (2007). "Analysis of the flexural response of NSM FRP-strengthened
942 concrete beams." *Proceedings, 8th International Conference on Fibre Reinforced
943 Plastics for Reinforced Concrete Structures (FRPRCS-8)*, Patras, Greece, July 16 to 18,
944 2007 (CD-ROM).
- 945 [50] Novidis, D. G., and Pantazopoulo, S. J. (2007). "Beam tests of NSM – FRP laminates
946 in concrete." *Proceedings, 8th International Conference on Fibre Reinforced Plastics
947 for Reinforced Concrete Structures*, Patras, Greece, July 16-18, 2007 (CD-ROM).
- 948 [51] Thorenfeldt, E. (2007). "Bond capacity of CFRP strips glued to concrete in sawn slits."
949 *Proceedings, 8th International Conference on Fibre Reinforced Plastics for Reinforced
950 Concrete Structures*, Patras, Greece, July 16 to 18, 2007 (CD-ROM).
- 951 [52] Kalayci, A.S., Yalim, B. and Mirmiran, A. (2010). "Construction tolerances and design
952 parameters for NSM FRP reinforcement in concrete beams." *Construction and Building
953 Materials*, 24(10), 1821-1829.
- 954 [53] Dalfre, G.M. and Barros, J.A.O. (2011). "Flexural Strengthening of RC Continuous
955 Slab Strips Using NSM CFRP Laminates." *Advances in Structural Engineering*, 14(6),
956 1223-1245.
- 957 [54] Peng, H., Zhang, J.R., Cai, C.S. and Liu, Y. (2014). "An experimental study on
958 reinforced concrete beams strengthened with prestressed near surface mounted CFRP
959 strips." *Engineering Structures*, 79, 222-233.
- 960 [55] Sharaky, I.A., Torres, L. and Sallam, H.E.M. (2015). "Experimental and analytical
961 investigation into the flexural performance of RC beams with partially and fully bonded
962 NSM FRP bars/strips." *Composite Structures*, 122, 113-126.
- 963 [56] Capozucca, R., Bossoletti, S., and Montecchiani, S. (2015). "Assessment of RC beams
964 with NSM CFRP rectangular rods damaged by notches." *Composite Structures*, 128,
965 322-341.
- 966 [57] Wu, G., Dong, Z.Q., Wu, Z.S. and Zhang, L.W. (2014). "Performance and parametric

- 967 analysis of flexural strengthening for RC beams with NSM-CFRP bars.” *Journal of*
 968 *Composites for Construction*, 18 (4), DOI: 10.1061/(ASCE)CC.1943-5614.0000451.
- 969 [58] Fernandes, P.M.G., Silva, P.M. and Sena-Cruz, J. (2015). “Bond and flexural behavior
 970 of concrete elements strengthened with NSM CFRP laminate strips under fatigue
 971 loading.” *Engineering Structures*, 84, 350-361.
- 972 [59] Barros, J.A.O., Costa, I.G. and Ventura-Gouveia, A. (2011). “CFRP Flexural and Shear
 973 Strengthening Technique for RC Beams: Experimental and Numerical Research.”
 974 *Advances in Structural Engineering*, 14(3), 551-573.
- 975 [60] Nanni, A., Bakis, C. E., and Boothby, T. E. (1995). “Test methods for FRP-concrete
 976 systems subjected to mechanical loads: state of the art review.” *Journal of Reinforced*
 977 *Plastics and Composites*, 14(6), 524-558.
- 978 [61] Blaschko, M. (2003). “Bond behaviour of CFRP strips glued into slits.” *Proceedings,*
 979 *6th International Symposium on Fibre-Reinforced Polymer (FRP) Reinforcement for*
 980 *Concrete Structures*, July8-10, 2003, Singapore, p.205-214.
- 981 [62] Yan, X., Miller, B., Nanni, A., and Bakis, C. E. (1999). “Characterization of CFRP bars
 982 used as near-surface mounted reinforcement.” *Proceedings, 8th International Structural*
 983 *Faults and Repair Conference*, Edinburgh (Scotland), 1999 (CD-ROM).
- 984 [63] Li, R., Teng, J. G., and Yue, Q. R. (2005). “Experimental study on bond behavior of
 985 NSM CFRP strips-concrete Interface.” *Industrial Construction*, 35(8), 31-35 (in
 986 Chinese).
- 987 [64] Shield, C. K., French, C. W., and Milde, E. (2005). “The effect of adhesive type on the
 988 bond of NSM tape to concrete.” *ACI SP230: the 7th International Symposium on*
 989 *Fiber-Reinforced Polymer (FRP) Reinforcement for Concrete Structures*, American
 990 *Concrete Institute*, November, p.355-372.
- 991 [65] Rashid, R., Oehlers, D. J., and Seracino, R. (2008). “IC debonding of FRP NSM and
 992 EB retrofitted concrete: plate and cover interaction tests.” *Journal of Composites for*
 993 *Construction*, 12(2), 160-167.
- 994 [66] Kotynia, R. (2012). “Bond between FRP and concrete in reinforced concrete beams
 995 strengthened with near surface mounted and externally bonded reinforcement.”
 996 *Construction and Building Materials*, 32, 41-54.
- 997 [67] Teng, J.G., Zhang, S.S., Dai, J.G. and Chen, J.F. (2013). “Three-dimensional
 998 meso-scale finite element modeling of bonded joints between a near-surface mounted
 999 FRP strip and concrete.” *Computers & Structures*, 117, 105-117.
- 1000 [68] Dai, J.G., Ueda, T., Sato, Y. (2005). “Development of the nonlinear bond stress-slip
 1001 model of fiber reinforced plastics sheet-concrete interfaces with a simple method.”
 1002 *Journal of Composites for Construction*, 9(1), 52-62.
- 1003 [69] Lu, X.Z., Teng, J.G., Ye, L.P., Jiang, J.J. (2005). “Bond-slip models for FRP
 1004 sheets/plates bonded to concrete.” *Engineering Structures*, 27(6), 920-937.
- 1005 [70] Sena Cruz, J. M., and Barros, J. A. O. (2004). “Bond between near-surface mounted
 1006 carbon-fiber-reinforced polymer laminate strips and concrete.” *Journal of Composites*
 1007 *for Construction*, ASCE, 8(6), 519-527.
- 1008 [71] De Lorenzis, L., and Nanni, A. (2002). “Bond between near-surface mounted
 1009 fiber-reinforced polymer rods and concrete in structural strengthening.” *ACI Structural*
 1010 *Journal*, 99(2), 123-132.
- 1011 [72] De Lorenzis, L., Lundgren, K., and Rizzo, A. (2004). “Anchorage length of
 1012 near-surface mounted fibre-reinforced polymer bars for concrete
 1013 strengthening-experimental investigation and numerical modeling.” *ACI Structural*
 1014 *Journal*, 101(2), 269-278.
- 1015 [73] De Lorenzis, L., Rizzo, A., and La Tegola, A. (2002). “A Modified pull-out test for
 1016 bond of near-surface mounted FRP rods in concrete.” *Composites Part B: Engineering*,

- 1017 33(8), 589-603.
- 1018 [74] Sena Cruz, J. M., and Barros, J. A. O. (2004). "Modeling of bond between near-surface
1019 mounted CFRP laminate strips and concrete." *Computers and Structures*, 82(17-19),
1020 1513-1521.
- 1021 [75] Eligehausen, R. Popov, E.P. and Bertero, V.V. (1983). "Local bond stress-slip
1022 relationships of deformed bars under generalized excitations." Report No. 83/23, EERC,
1023 Berkeley, CA: University of California.
- 1024 [76] CEB-FIP. (1993). "Model Code 90." Lausanne; 1993.
- 1025 [77] Teng, J. G., Zhang, S. S., and Dai, J. G. (2009). "Finite element modelling of FRP strips
1026 near-surface mounted to concrete." *Proceedings, 9th International Symposium on*
1027 *Fiber-Reinforced Polymers Reinforcement for Concrete Structures (FRPRCS-9)*, July
1028 13-15, 2009, Sidney, Australia (CD-ROM).
- 1029 [78] Chen, J.F. and Teng, J.G. (2001). "Anchorage strength models for FRP and steel plates
1030 bonded to concrete." *Journal of Structural Engineering, ASCE*, 127(7), 784-791.
- 1031 [79] Yao, J., Teng, J.G. and Chen, J.F. (2005). "Experimental study on FRP-to-concrete
1032 bonded joints." *Composites Part B: Engineering*, 36(2), 99-113.
- 1033 [80] Yuan, H., Teng, J.G., Seracino, R., Wu, Z.S., and Yao, J. (2004). "Full-range behavior
1034 of FRP-to-concrete bonded joints." *Engineering Structures*, 26(5), 553-565.
- 1035 [81] Yuan, H., Wu, Z.S., and Yoshizawa, H. (2001). "Theoretical solutions on interfacial
1036 stress transfer of externally bonded steel/composite laminates." *Journal of Structural*
1037 *Mechanics and Earthquake Engineering, JSCE*, 18(1), 27-39.
- 1038 [82] Bianco, V., Barros, J.A.O. and Monti, G. (2009). "Bond Model of NSM FRP strips in
1039 the context of the Shear Strengthening of RC beams", *Journal of Structural*
1040 *Engineering - ASCE*, 135(6), 619-631.
- 1041 [83] Bianco, V., Barros, J.A.O. and Monti, G. (2010). "New approach for modeling the
1042 contribution of NSM FRP strips for shear strengthening of RC beams", *Journal of*
1043 *Composites for Construction - ASCE*, 14(1), 36-48.
- 1044 [84] Dalfré, G. and Barros, J.A.O. (2013). "NSM technique to increase the load carrying
1045 capacity of continuous RC slabs", *Engineering Structures*, 56, 137-153.
- 1046 [85] Breveglieri, M., Barros, J.A.O., Dalfré, G.M. and Aprile, A. (2013). "A parametric
1047 study on the effectiveness of the NSM technique for the flexural strengthening of
1048 continuous RC slabs", *Composites Part B-Engineering*, 43(4), 1970-1987.
- 1049 [86] Sena Cruz, J., Barros, J.A.O., Bianco, V., Bilotta, A., Bournas, D., Ceroni, F., Dalfré, G.,
1050 Kotynia, R., Monti, G., Nigro, E. and Triantafillou, T. (2016). *NSM Systems, Design*
1051 *Procedures for the Use of Composites in Strengthening of Reinforced Concrete*
1052 *Structures: State-of-the-Art Report of the RILEM Technical Committee 234-DUC (pp.*
1053 *303-348)*. Dordrecht: Springer Netherlands.
- 1054 [87] Firmo, J.P. and Correia, J.R. (2016). "Fire behaviour of thermally insulated RC beams
1055 strengthened with NSM-CFRP strips: Experimental study", *Composites Part*
1056 *B-Engineering*, 76, 112-121.
- 1057 [88] Benedetti, A., Fernandes, P., Granja, J.L., Sena-Cruz, J. and Azenha, M. (2016).
1058 "Influence of temperature on the curing of an epoxy adhesive and its influence on bond
1059 behaviour of NSM-CFRP systems", *Composites Part B-Engineering*, 89, 219-229.
- 1060 [89] Yu, B.L. and Kodur, V. (2014). "Effect of temperature on strength and stiffness
1061 properties of near-surface mounted FRP reinforcement", *Composites Part*
1062 *B-Engineering*, 58, 510-517.
- 1063 [90] Zhu, H., Wu, G., Zhang, L., Zhang, J.F. and Hui, D. (2014). "Experimental study on the
1064 fire resistance of RC beams strengthened with near-surface-mounted high-T-g BFRP",
1065 *Composites Part B-Engineering*, 60, 680-687.
- 1066 [91] Teng, J. G., Yuan, H. and Chen, J. F. (2006). "FRP-to-concrete interfaces between two

- 1067 adjacent cracks: Theoretical model for debonding failure.” *International Journal of*
 1068 *Solids and Structures*, 43(18–19), 5750–5778.
- 1069 [92] Oehlers, D. J., Liu, I. S. T., Seracino, R. (2005). “Shear deformation debonding of
 1070 adhesively bonded plates.” *Structures & Buildings*, 158(Issue SB1), 77–84.
- 1071 [93] Oehlers, D. J., Liu, I. S. T., Seracino, R., and Ali, M. S. M. (2004). “Prestress model for
 1072 shear deformation debonding of FRP- and steel-plated RC beams.” *Magazine of*
 1073 *Concrete Research*, 56(8), 475-486.
- 1074 [94] Teng, J. G., and Yao, J. (2007). “Plate end debonding in FRP-plated RC beams-II:
 1075 strength model.” *Engineering Structures*, 29(10), 2472-2486.
- 1076 [95] Malek, A. M., Saadatmanesh, H., and Ehsani, M. R. (1998). “Prediction of failure load
 1077 of R/C beams strengthened with FRP plate due to stress concentration at the plate end.”
 1078 *ACI Structural Journal*, 95(1), 142-152.
- 1079 [96] Zhang, J. P. (1997). “Diagonal cracking and shear strength of reinforced concrete
 1080 beams.” *Magazine of Concrete Research*, 49(178), 55-65.
- 1081 [97] Zhang, S., Raof, M., and Wood, L. A. (1995). “Prediction of peeling failure of
 1082 reinforced-concrete beams with externally bonded steel plates.” *Proceedings, the*
 1083 *Institution of Civil Engineers-Structures and Buildings*, 110(3), 257-268.
- 1084 [98] Wang, C.Y. and Ling, F.S. (1998). “Prediction model for the debonding failure of
 1085 cracked RC beams with externally bonded FRP sheets.” *Proceedings, 2nd International*
 1086 *Conference of Composites in Infrastructure (ICCI)*, 1998, Arizona, USA, p. 548–562.
- 1087 [99] De Lorenzis, L., and Nanni, A. (2003). “Proposed design procedure of NSM FRP
 1088 reinforcement for strengthening of RC beams.” *Proceedings, 6th International*
 1089 *Symposium on FRP Reinforcement for Concrete Structures*, Singapore, 1455-1464.
- 1090 [100] Raof, M., and Zhang, S. (1997). “An insight into the structural behaviour of reinforced
 1091 concrete beams with externally bonded plates.” *Proceedings of the Institution of Civil*
 1092 *Engineers-Structures and Buildings*, 122(4), 477-492.
- 1093 [101] Hussain, M., Sharif, A., Basunbul, I. A., Baluch, M. H. and Alsulaimani, G. J. (1995).
 1094 “Flexural behavior of precracked reinforced-concrete beams strengthened externally by
 1095 steel plates”, *ACI Structural Journal*, 92(1), 14-22.
- 1096 [102] Sallam, H.E.M., Saba, A.M., Shahin, H.H. and Abdel-Raouf, H. (2004). “Prevention of
 1097 peeling failure in plated beams”, *Journal of Advanced Concrete Technology*, 2(3),
 1098 419–429.
- 1099 [103] Demakos, C. and Koutsoukos, D. (2003). “Effective strengthening of reinforced
 1100 concrete beams with anchored FRPs”, *Recent Advances in Composite Materials*.
 1101 Springer.
- 1102 [104] Smith, S. T. and Teng, J.G. (2003). “Shear-bending interaction in debonding failures of
 1103 FRP-plated RC beams”, *Advances in Structural Engineering*, 6(3), 183–99.
- 1104 [105] Piamanmas, A. and Pornpongsaroj, P. (2004). “Peeling behaviour of reinforced concrete
 1105 beams strengthened with CFRP plates under various end restraint conditions”,
 1106 *Magazine of Concrete Research*, 56(2), 73-81.
- 1107 [106] Kalfat, R., Al-Mahaidi, R. and Smith, S.T. (2013). “Anchorage devices used to improve
 1108 the performance of reinforced concrete beams retrofitted with a FRP composites:
 1109 State-of-the-art review”, *Journal of Composites for Construction*, ASCE, 17(1), 14-33.
- 1110 [107] Grelle, S.V. and Sneed, L.H. (2013). “Review of anchorage systems for
 1111 externally-bonded FRP laminates”, *International Journal of Concrete Structures and*
 1112 *Materials*, 7(1), 17–33
- 1113 [108] Skuturna, T. and Valivonis, J. (2016). “Experimental study on the effect of anchorage
 1114 systems on RC beams strengthened using FRP”, *Composites Part B-Engineering*, 91,

- 1115 283-290.
1116 [109] Hosen, M., Jumaat, M.Z. and Islam, S. (2015). "Inclusion of CFRP-Epoxy Composite
1117 for End Anchorage in NSM-Epoxy Strengthened Beams", *Advances in Materials
1118 Science and Engineering*, 2015.
1119
1120

ACCEPTED MANUSCRIPT

Figures

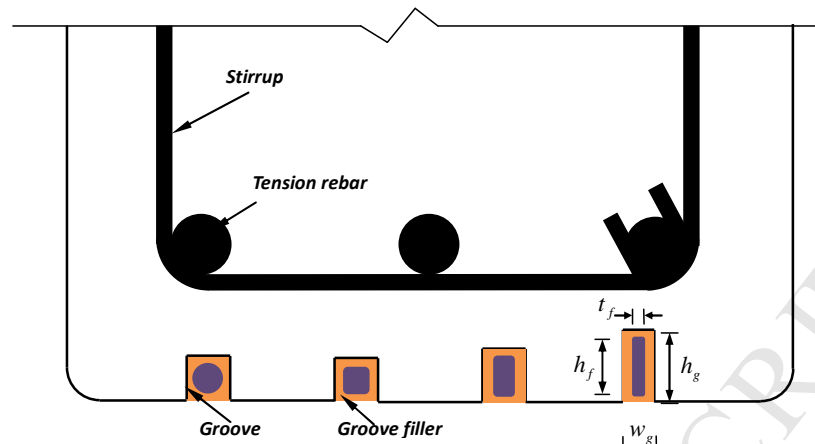


Fig. 1. Schematic of NSM FRP strengthening systems

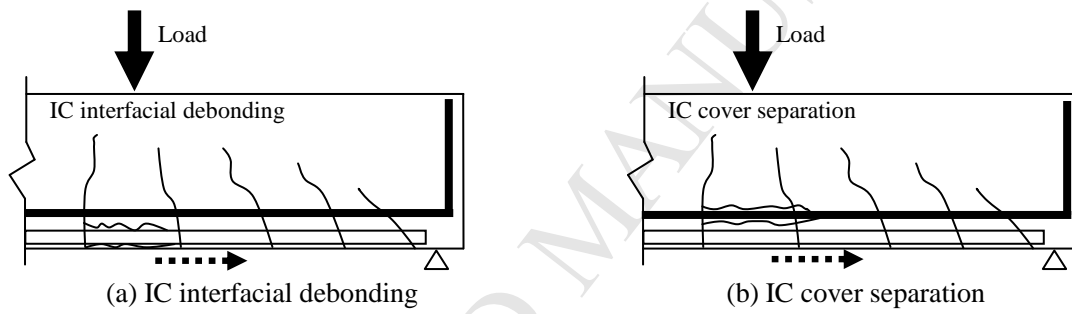


Fig. 2. Schematic of the IC debonding

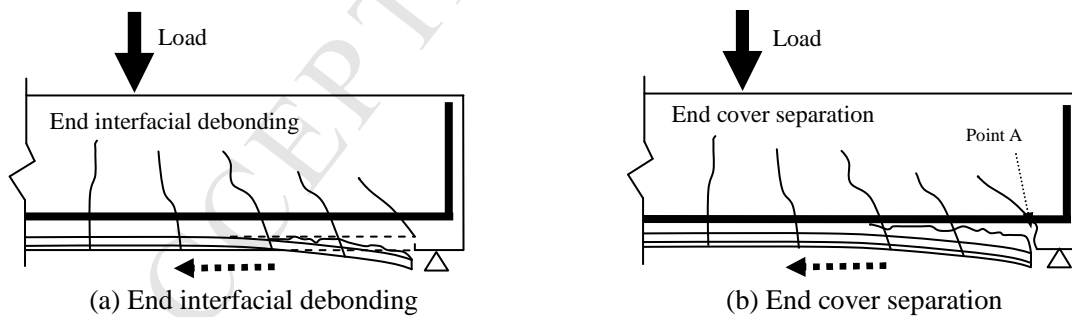


Fig. 3. Schematic of the end debonding

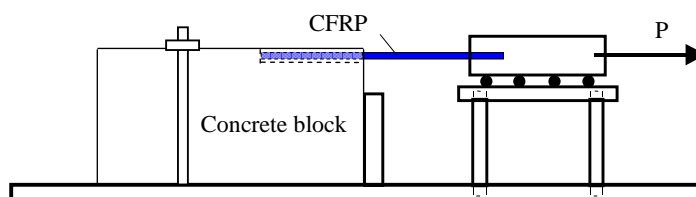


Fig. 4. Test setup of NSM FRP bonded joints

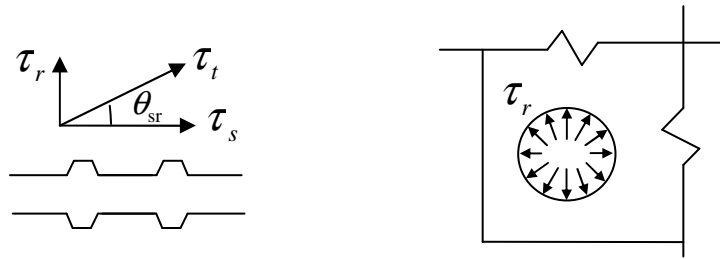


Fig. 5. Bond stresses between steel and concrete

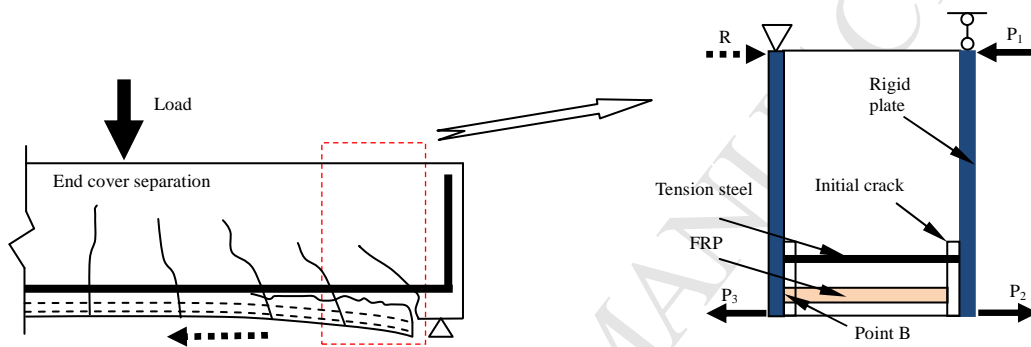


Fig. 6. Simplified FE model